

Thermal Fatigue Analyses of Riveted Structures

Eyüp YETER

Gaziantep University, Aeronautics and Aerospace Faculty, Aircraft and Aerospace Engineering Department, Gaziantep, Turkey, E-mail: eyeter@gantep.edu.tr

crossref <http://dx.doi.org/10.5755/j01.mech.24.5.21288>

1. Introduction

Due to the nature of the aviation industry, it has become imperative to use light and strength materials in the design of constructions used in this area. This necessity requires the use of aluminum alloys or polymer matrix composites in the industry. Aluminum alloys and composite materials are predominantly used in the outer surfaces of aircraft and in the connection components on the outer surface. These structures are usually connected by mechanical connections or by using various adhesives. Riveted connections are the most commonly used ones among the mechanical connections.

Fatigue is the local and progressive structural damages of materials under the cyclic and variable loading conditions. Thermal fatigue, a type of fatigue, is the result of cyclic temperature changes depending on the operating conditions of materials, causing in the formation of micro-cracks on the surface of the materials and these micro-cracks propagations cause structural damages to the structure. The materials used in the aviation sector are subjected to continuous and cyclic temperature changes due to their operating conditions. The thermal loadings occur between the subzero and above zero temperatures. Thermal loading intensity and period, which are difficult to predict during the design stage, may cause damages on the materials and deterioration on the structures. The investigation of the formation of thermal fatigue and its effects on the different materials is important in terms of safety and costs.

The structures in the aviation industry are affected at a high rate from the thermal fatigue because it is usually necessary to use thin plates in the design of these structures to reduce the weight. Therefore, the researches in this concern are important to prevent or minimize the damage caused by this type of loadings. When the literature is examined, it is seen that generally thermal fatigue properties are examined between high temperatures above zero degrees. Lee et al. [1] investigated between ambient temperature and + 177 °C, Persson et al. [2, 3] between 170 °C and 650-850 °C, Paffumi et al. [4] between ambient temperature and 300-550 °C, Toshio Ramanujam et al. [5] between ambient temperature and 140 °C. In addition, in some studies, the thermal fatigue characteristics have been examined for restricted materials for below and above zero degrees [6-13]. Both metal (especially steel) and composite materials are researched. In one study, it was shown that carbon fiber reinforced polymer composites were not resistant to thermal fatigue [14]. Since the fiber and matrix used in the polymer composites have different coefficients of thermal expansion, the formation of high thermal stresses occurs.

Bhattachar [15] researched the thermal fatigue characteristics of nickel-based super alloy 263. Influences

of variations of thicknesses examined and the number of cycles at which crack initiated was investigated. Results have shown that thickness didn't have important influences on the thermal fatigue resistance. Effects of thermal cycles on the crack initiation and propagation of 316 L steel have been researched by Fissolo et al. [16] and Robertson et al. [17]. Effects of thermal fatigue on crack initiation and growth of AISI 304L stainless steel was investigated by Haddar et al. [18]. A model to predict the crack network propagation under thermal loads was constructed. Thermal fatigue analyses of cast irons used in the automotive industry have been performed by Mellouli et al. [19]. Influences of temperature, microstructure and chemical compositions of used material types on starting of crack and propagation of crack with the effects of thermal cycles were studied. Agbadua et al. [20] investigated the thermal fatigue resistance of low carbon steels. Composition analyses were conducted to determine the carbon ratio in the received materials. Moon and Tae Kwon [21] studied thermal fatigue characteristics of stainless steel (300 series). It was shown that thermal fatigue durability of STS 304 was better among the 300 series stainless steels. Mechanisms of thermal fatigue and phase change of steels used in brake discs were analyzed by Li et al. [22]. Initiation and growth of thermal cracks with the effects of hard braking processes were examined.

Szmytka et al. [23] studied thermal fatigue analyses of automotive diesel piston by experimentally and numerically. A fatigue criterion for aluminum alloys were proposed to predict the life of the piston under cyclic loading. Thermal mechanical fatigue characteristics of single crystal super alloy were researched by Segersall et al. [24]. Influences of alloying with Si or Re were explained. Kwon et al. [25] studied on the damage analyses of wheels which exposed thermal loads. Metallurgical transformation analysis, hardness analysis, and the residual stress analysis were performed. Finite element (FE) analyses were also conducted. It was shown that the hardness of thermally damaged region was higher than the non-damaged wheel. Yeter [26] studied the thermal fatigue characteristics of materials used in aerospace structures. Thermal fatigue resistance of tool steels was determined by Chen et al. [27]. Firstly, thermal fatigue tests were performed to observe thermal cracks using induction heating and water cooling cyclically. Then, FE analyses were conducted by using data observed from experimental study and energy-based model.

The literature review showed that it is generally seen that thermal fatigue properties are examined between high temperatures above zero degrees. No studies have been done on the effects of thermal fatigue on riveting parameters. In this study, effects of thermal fatigue on the riveting parameters for 2014, 2024, 6061 and 7075 aluminum alloys which are widely used in the aviation industry have been

investigated. An algorithm has been developed under ANSYS finite element analysis software to determine the behavior of these structures that are exposed repeated thermal loading. The rivet spacing (RS), the rivet edge distance (ED) and the rivet hole diameter (RD) were selected as riveting parameters. It is aimed to determine the optimum values of the parameters used under thermal fatigue loading and the most suitable one for this loading among the materials used.

2. Materials and methods

In this study, the effects of thermal fatigue loading on the riveting parameters with the aid of an algorithm developed under ANSYS finite element analysis software. The flow chart used in this algorithm is given in Fig. 1. This algorithm is based on the principle of determining the distribution of the safety factor on the material subjected to the thermal fatigue load. As given in the flowchart, a fatigue failure theory is used in designing for fatigue life. The Soderberg failure theory, which is the more conservative theory, was used in this study. For Soderberg failure theory, the Eq. (1) is used to obtain safety factor:

$$n = \frac{1}{\frac{S_a}{S_e} + \frac{S_m}{S_y}}, \quad (1)$$

where: n is Safety factor, S_a is Alternating stress, S_m is Mean stress, S_e is Endurance strength, S_y is Yield strength.

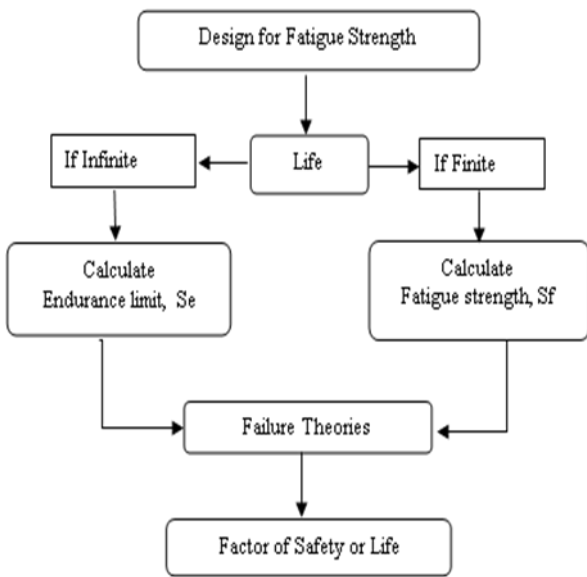


Fig. 1 Flowchart for design for fatigue strength

In the algorithm, the alternating stress and mean stress are calculated using data obtained after cyclic thermal loading. Then, safety factor distribution of materials is calculated using the other information of materials such as endurance strength and yield strength using eq. (1). Thin plate having 144x144x2 mm dimensions is used as case study. 3/32" (2.38 mm), 1/8" (3.17 mm), 5/32" (3.96 mm) and 3/16" (4.76 mm) rivet diameters were selected since they are commonly used ones. The rivet drill diameters to be opened for these rivet diameters are 2.5 mm, 3.2 mm, 4 mm and 4.8

mm, respectively. The rivet drill diameter (rivet hole diameter) was selected to be 3.2 mm when the rivet diameter was considered constant in the study and the effects of other riveting parameters were investigated. In the study, the rivet spacing (RS), the rivet edge distance (ED) and the rivet hole diameter (RD) were selected as riveting parameters.

In order to inspect the thermal stresses of the plates with riveting parameters, the SHELL181 element type is used. SHELL181 is suitable for analyzing thin to moderately-thick shell structures. It is a four-node element with six degrees of freedom at each node: translations in the x, y, and z directions, and rotations about the x, y, and z-axes. SHELL181 is well-suited for linear, large rotation, and/or large strain nonlinear applications. Temperatures can be input as element body loads at the corners of the outside faces of the element and at the corners of the interfaces between layers [28]. In this study, the uniform temperature was assigned to the nodes considering reference temperature as 25°C. Like a structural analysis under the mechanical loads, the thermal strains are obtained after each load cycle. Surface of the element can be subjected to both maximum tension and maximum compression stresses in one full rotation. This type of loads creates fatigue on the structures and known as reversed type stress. In the study, reversed type fatigue loading was used. Firstly, +70°C uniform temperature load was applied and then the plate subjected to -70°C thermal load (no extra mechanic loads are applied to see the direct effects of thermal loads). Thermal strains are obtained for both types of loadings. The safety factor distributions of plates were predicted using the failure criteria, obtained stresses from thermal strains, and the other material properties. Rivet pins are considered rigid. The plate is fixed from the pin holes (Fig. 2) providing no translations in the x, y, and z directions, and no rotations about the x, y, and z-axes. The material properties of the used aluminum alloys are given in Table 1. These material properties, determined in standard conditions (room-temperature), are taken from a strength of materials textbook [29].

As given in Fig 1, there are two alternatives for the design for fatigue strength; design for finite or infinite life. If the life is chosen as infinite (in this study it was chosen) endurance strength is used. In experimental fatigue strength studies, the structures are exposed to the cycles under constant or increased stresses and life of the structure are obtained from cycle and stress information. For infinite fatigue predictions, it is considered that the structure can have at least 10^6 cycles. This approach was used in this numeric study. So, in this study, the safety factor distributions of structures can be obtained instead of maximum stress and cycle curves.

Table 1

Material Properties

Material	Yield stress σ_y , MPa	Young's modulus E , MPa	Modulus of Rigidity G , GPa	Poisson's ratio, ν	Thermal expansion coefficient α , °C ⁻¹
Al 7075 T6	500	72	28	0.3	23.6x10 ⁻⁶
Al 6061 T6	240	70	26	0.3	23.6x10 ⁻⁶
Al 2024 T4	325	73	27	0.3	23.2x10 ⁻⁶
Al 2014 T6	400	75	27	0.3	23.0x10 ⁻⁶

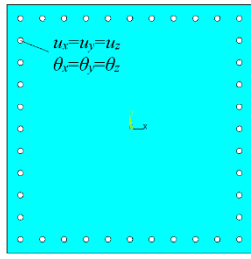


Fig. 2 Boundary conditions

Furthermore, d, RS, ED and Rd abbreviations stand for rivet diameter, rivet spacing, rivet edge distance and rivet hole diameter, respectively as shown in Fig. 3.

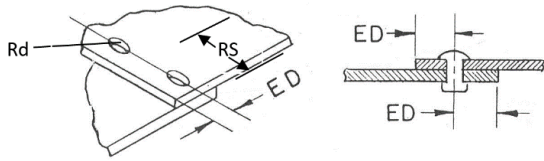


Fig. 3 Riveting parameters

3. Results and discussions

Aim of this study is to predict thermal fatigue resistance of various Al Alloys (7075 T6, 6061 T6, 2024 T4 and 2014 T6) by means of safety factor distributions on the structures that are exposed to the cyclic thermal loading and to find effects of thermal fatigue on riveting parameters. The rivet spacing (RS), the rivet edge distance (ED) and the rivet hole diameter (RD) were selected as riveting parameters. It is aimed to determine the optimum values of the parameters used under thermal fatigue loading and the most suitable one for this loading among the materials used.

3.1. Effects of rivet spacing

The rivet spacing is the distance between the centers of the rivets on the same row of the plate. When investigating the effects of the rivet spacing on thermal fatigue resistance of structures, the rivet spacing is changed to be 3 times (3 d), 4 times (4 d), 5 times (5 d), 6 times (6 d), 7 times (7 d), and 8 times (8 d) of used rivet diameter. In Fig. 4, the relationship between the change of rivet spacing and the change of minimum safety factor values for different aluminum types is given. As can be seen, the highest safety factor value for all material types is obtained when the rivet spacing is 3 times the rivet diameter.

It was known that the increase of rivet spacing under compressive loading causes the failure [30]. For thermal fatigue case, it is also seen that the plates under thermal fatigue load, the value of the safety factor decreases. In other words, the possibility of being a failure of structures are increased when RS is increased as shown in Fig. 4 and numerical values are given in the Table 2. It is seen from the Fig. 4 that safety factor decreases by changing rivet spacing from 3D to 8D for all material types. For all RS values, it was found that material 7075 has the highest safety coefficient distribution among aluminum alloys.

In Fig. 5, the distribution of the safety factor on the plate is given as an example, in the case of the RS equals to the 8d.

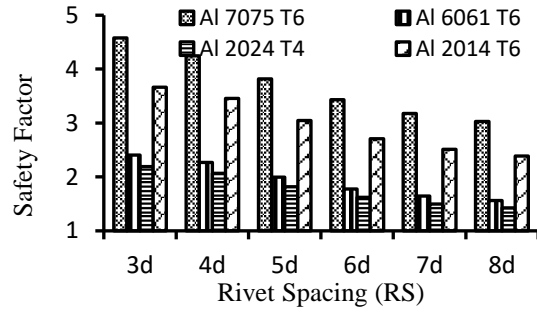


Fig. 4 Variation of minimum safety factor with rivet spacing

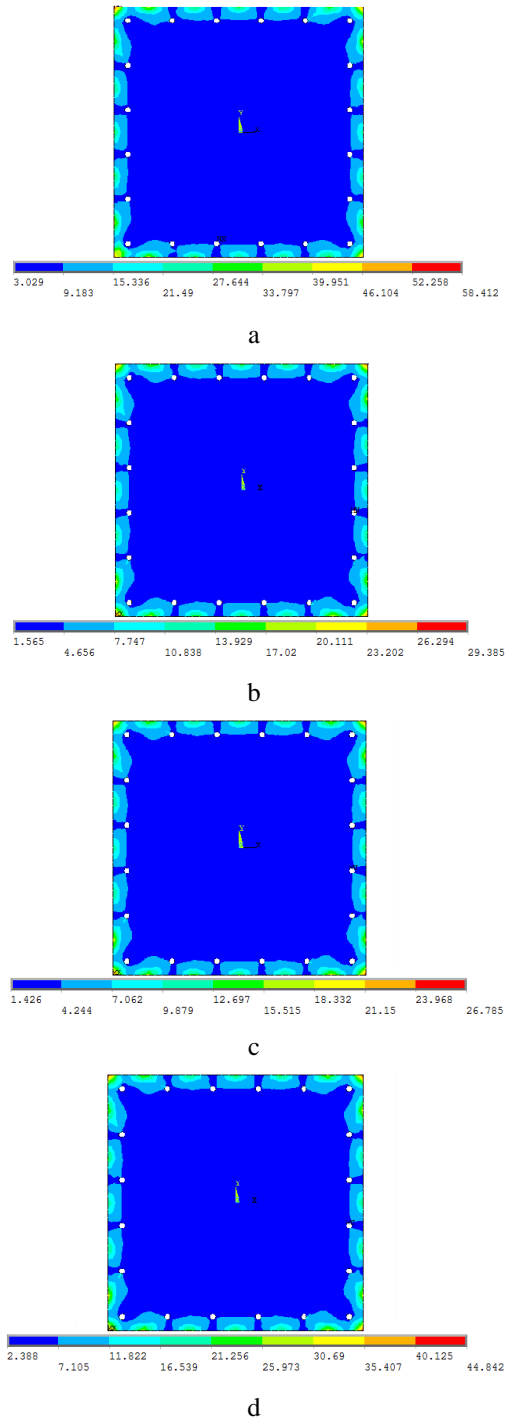


Fig. 5 Safety factor distribution of AL alloys with RS = 8d and ED=2.5d a) 7075T6, b) 6061T6, c) 2024T4, d) 2014T6

Table 2

Minimum safety factor values with rivet spacing

Rivet Spacing	Al 7075 T6	Al 6061 T6	Al 2024 T4	Al 2014 T6
3d	4.576	2.403	2.190	3.667
4d	4.249	2.267	2.066	3.459
5d	3.816	1.996	1.819	3.046
6d	3.432	1.776	1.619	2.711
7d	3.177	1.645	1.499	2.510
8d	3.029	1.565	1.426	2.388

3.2. Effects of rivet edge distance

The rivet edge distance is the distance from the center of the rivet to the edge of the plate. While the effects of the rivet edge distance (ED) on thermal fatigue were investigated, the rivet edge distance was considered to be 1 times (1 d), 2.5 times (2.5 d) and 5 times (5 d) of the rivet diameter used. While the effect of the rivet edge distance is researched, the rivet area and rivet hole diameter are assumed to be 3d and 3.2 mm, respectively. Fig. 6 and Table 3 show the relationship between the change in rivet edge distance and the change in minimum safety factor values for different types of aluminum. As was the case with mechanical loading [31], when the rivet edge distance increased from 1d to 2.5 d, the safety factor values increased for all material types. When the rivet edge distance is greater than 2.5 d, the value of the safety factor begins to decrease. For all ED values, it is seen that material 7075 has the highest safety factor distribution among the used aluminum alloys. Furthermore, it has been determined that the 2024 T4 alloy has the smallest value of safety factor.

Table 3

Minimum safety factor values with rivet Edge Distance

Rivet Edge Distance	Al 7075 T6	Al 6061 T6	Al 2024 T4	Al 2014 T6
1d	3.99	1.993	1.816	3.041
2.5d	4.552	2.413	2.199	3.682
5d	4.505	2.341	2.134	3.573

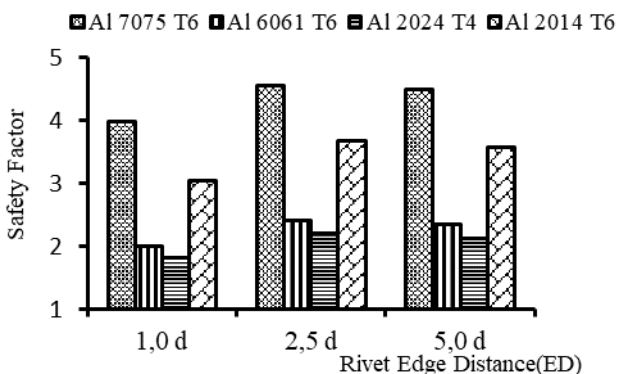


Fig. 6 Variation of minimum safety factor with rivet spacing

3.3. Effects of rivet hole diameter

While the effects of the size of the rivet hole on thermal fatigue were investigated, the rivet diameters used were chosen as 2.5 mm, 3.2 mm, 4 mm and 4.8 mm. The relationship between the variations of the minimum safety

factor values with respect to the variation of rivet diameters for different aluminum types is given in Fig. 7 and table 4. It is known that using bigger sizes of rivets increases the maximum mechanical load that can be carried by a thin plate [30]. It has been seen that when the rivet hole diameter is increased from 2.5 mm to 4.8 mm, the safety factor value increases with this change. For all rivet diameters, it is seen that material 7075 has the highest safety factor distribution among aluminum alloys. Moreover, it is seen that Al 2024 T4 alloy has the smallest safety factor value.

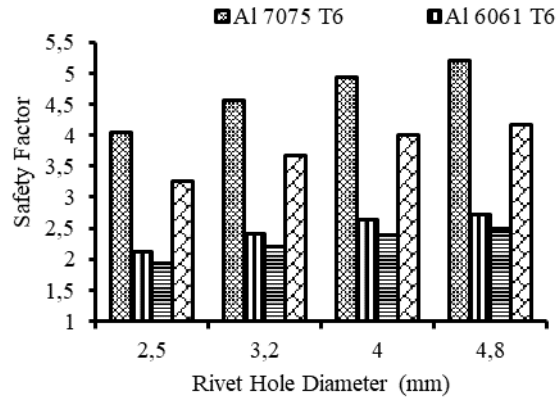


Fig. 7 Variation of minimum safety factor value with rivet hole diameter

Table 4

Minimum safety factor values with rivet hole Diameter

Rivet hole Diameter (mm)	Al 7075 T6	Al 6061 T6	Al 2024 T4	Al 2014 T6
2.5	4.042	2.128	1.940	3.248
3.2	4.552	2.413	2.199	3.682
4	4.937	2.628	2.396	4.011
4.8	5.207	2.725	2.484	4.159

4. Conclusions

In this study, thermal fatigue resistance of various Al Alloys (7075 T6, 6061 T6, 2024 T4 and 2014 T6) by means of safety factor distributions on the structures that are exposed to the cyclic thermal loading was investigated. And effects of riveting parameters on this resistance was researched. The rivet spacing (RS), the rivet edge distance (ED) and the rivet hole diameter (RD) were selected as riveting parameters. It is aimed to determine the optimum values of the parameters used under thermal fatigue loading and the most suitable one for this loading among the materials used. From the present study, the conclusions can be summarized as:

- It has been determined that when the rivet spacing is 3 times the rivet diameter (3d), the highest safety factor value is obtained for all material types and this value decreases when the rivet spacing is increased. In the case of rivet spacing is 3d, the safety factor value of 7075 T6 aluminum alloy is about 52% higher than 2024 T4. When the rivet spacing is increased from 3d to 8d, the safety factor value for the 7075 T6 aluminum alloy is reduced by about 34%.
- When the effect of the rivet edge distance is examined, it is seen that when the rivet edge distance 8d

is chosen, the highest safety factor value is obtained.

- When the rivet edge distance $2.5d$ is used, the safety value is the smallest. For $2.5d$ ED, the safety factor value of 7075 T6 aluminum alloy is about 49% higher than 2024 T4. When the rivet edge distance is increased from $1d$ to $5d$, the safety factor for the 7075 T6 aluminum alloy increases by 13%.
- In addition, rivet hole diameter increased from 2.5 mm to 4.8 mm, and safety factor value increased with this change. When the rivet hole diameter is equal to 4.8 mm, the Al 7075 T6 safety factor is about 44% higher than the Al 2024 T4.

References

1. **Lee, S. H.; Nam, J. D.; Ahn, K.; Chung, K. M.; Seferis, J.C.** 2001. Thermo-oxidative stability of high performance composites under thermal cycling conditions, *Journal of composite materials*, 35(5): 433-454. <https://doi.org/10.1177/002199801772662172>.
2. **Persson, A.; Hogmark, S.; Bergström, J.** 2004. Simulation and evaluation of thermal fatigue cracking of hot work tool steels, *International Journal of Fatigue*, 26(10): 1095-1107. <https://doi.org/10.1016/j.ijfatigue.2004.03.005>.
3. **Persson, A.; Hogmark, S.; Bergström, J.** 2005. Thermal fatigue cracking of surface engineered hot work tool steels, *Surface and Coatings Technology*, 191(2): 216-227. <https://doi.org/10.1016/j.surfcoat.2004.04.053>.
4. **Paffumi, E.; Nilsson, K.-F.; Szaraz, Z.** 2015. Experimental and numerical assessment of thermal fatigue in 316 austenitic steel pipes, *Engineering Failure Analysis*, 47: 312-327. <https://doi.org/10.1016/j.engfailanal.2014.01.010>.
5. **Ramanujam, N.; Vaddadi, P.; Nakamura, T.; Singh, R.P.** 2008. Interlaminar fatigue crack growth of cross-ply composites under thermal cycles, *Composite Structures*, 85(2): 175-187. <https://doi.org/10.1016/j.compstruct.2007.10.018>.
6. **Deteresa, S.; Nicolais, L.** 1988. The contribution of thermal stresses to the failure of Kevlar fabric composites, *Polymer composites*, 9(3): 192-197. <https://doi.org/10.1002/pc.750090305>.
7. **Kern, K.; Long Jr, E.; Long, S.** 1990. Effects of Electron Radiation and Thermal Cycling on Sized and Un-sized Carbon Fiber--Polyetherimide Composites, *Polym. Prepr.*, 31(1): 611-612. Available from Internet: <https://www.researchgate.net/publication/282382669>.
8. **Papadopoulos, D. S.; Bowles, K.J.** 1990. Use of unbalanced laminates as a screening method for microcracking, in *National SAMPE Symposium and Exhibition (Proceedings)*. Available from Internet: <https://ntrs.nasa.gov/search.jsp?R=19900011808>.
9. **Simpson, M.; Jacobs, P.; Jones, F.** 1991. Generation of thermal strains in carbon fibre-reinforced bismaleimide (PMR-15) composites: Part 1: The determination of residual thermal strains in cross-ply laminates, *Composites*, 22(2): 89-97. [https://doi.org/10.1016/0010-4361\(91\)90666-5](https://doi.org/10.1016/0010-4361(91)90666-5).
10. **Jacobs, P.; Simpson, M.; Jones, F.** 1991. Generation of thermal strains in carbon fibre-reinforced bismaleimide (PMR-15) composites: Part 2: The effect of volatiles, *Composites*, 22(2): 99-104. [https://doi.org/10.1016/0010-4361\(91\)90667-6](https://doi.org/10.1016/0010-4361(91)90667-6).
11. **Simpson, M.; Jacobs, P.; Jones, F.** 1991. Generation of thermal strains in carbon fibre-reinforced bismaleimide (PMR-15) composites: Part 3: A simultaneous thermogravimetric mass spectral study of residual volatiles and thermal microcracking, *Composites*, 22(2): 105-112. [https://doi.org/10.1016/0010-4361\(91\)90668-7](https://doi.org/10.1016/0010-4361(91)90668-7).
12. **Eggers, H.; Hartung, W.; Knaak, S.** 1991. Damage in carbon fibre reinforced epoxy after thermal cycling and T-fatigue loading, *Cryogenics*, 31(4): 265-268. [https://doi.org/10.1016/0011-2275\(91\)90090-J](https://doi.org/10.1016/0011-2275(91)90090-J).
13. **Potter, B.; Yuan, F.; Pater, R.** 1993. The effect of molecular weight on transverse microcracking in high-temperature LaRC-RP46T polyimide composites, *Journal of advanced materials*, 25(1): 30-34. Available from Internet: <https://www.researchgate.net/publication/282406149>.
14. **Kessler, S.S.; Matuszeski, T.; McManus, H.** 1998. Cryocycling and Mechanical Testing of CFRP for X-33 Liquid H2 Fuel Tank Structure, Technology Laboratory for Advanced Composites, Department of Aeronautics and Astronautics, Massachusetts Institute of Technology. Available from Internet: <http://www.metisdesign.com/docs/papers/62X-98.pdf>
15. **Bhattachar, V.** 1995. Thermal fatigue behaviour of nickel-base superalloy 263 sheets, *International journal of fatigue*, 17(6): 407-413. [https://doi.org/10.1016/0142-1123\(95\)00006-F](https://doi.org/10.1016/0142-1123(95)00006-F).
16. **Fissolo, A.; Marini, B.; Nais, G.; Wident, P.** 1996. Thermal fatigue behaviour for a 316 L type steel, *Journal of nuclear materials*, 233: 156-161. [https://doi.org/10.1016/S0022-3115\(96\)00122-5](https://doi.org/10.1016/S0022-3115(96)00122-5).
17. **Robertson, C.; Fivel, M.; Fissolo, A.** 2001. Dislocation substructure in 316L stainless steel under thermal fatigue up to 650 K, *Materials Science and Engineering: A*, 315(1): 47-57. [https://doi.org/10.1016/S0921-5093\(01\)01201-1](https://doi.org/10.1016/S0921-5093(01)01201-1).
18. **Haddar, N.; Fissolo, A.; Maillot, V.** 2005. Thermal fatigue crack networks: an computational study, *International Journal of Solids and Structures*, 42(2): 771-788. <https://doi.org/10.1016/j.ijsolstr.2004.06.033>.
19. **Mellouli, D.; Haddar, N.; Köster, A.; Toure, A.M.-L.** 2011. Thermal fatigue of cast irons for automotive application, *Materials & Design*, 32(3): 1508-1514. <https://doi.org/10.1016/j.matdes.2010.10.025>.
20. **Agbadua, S. A.; Mgbemena, C.O.; Mgbemena, C.E.; and Chima, L.O.** 2011. Thermal Cycling Effects on the Fatigue Behaviour of Low Carbon Steel. *Journal of Minerals and Materials Characterization and Engineering*, 10 (14): 1345-1357. <https://doi.org/10.4236/jmmce.2011.1014106>.
21. **Moon, J. H.; Ha, T.K.** 2014. Thermal fatigue behavior of austenitic stainless steels, *World Academy of Science Engineering and Technology*, *International Journal of Chemical, Molecular, Nuclear, Materials and Metallurgical Engineering*, 8(5): 394-7. [urn:dai:10.1999/1307-6892/9998126](https://doi.org/10.1999/1307-6892/9998126).
22. **Li, Z.; Han, J.; Yang, Z.; Li, W.** 2015. Analyzing the mechanisms of thermal fatigue and phase change of steel used in brake discs, *Engineering Failure Analysis*, 57: 202-218. <https://doi.org/10.1016/j.engfailanal.2015.07.002>.
23. **Szmytka, F.; Salem, M.; Rézai-Aria, F.; Oudin, A.**

2015. Thermal fatigue analysis of automotive diesel piston: Experimental procedure and numerical protocol, *International Journal of Fatigue*, 73: 48-57.
<https://doi.org/10.1016/j.ijfatigue.2014.11.011>.
24. **Segersäll, M.; Kontis, P.; Pedrazzini, S.; Bagot, P. A.; Moody, M. P.; Moverare, J. J.; Reed, R. C.** 2015. Thermal–mechanical fatigue behaviour of a new single crystal superalloy: effects of Si and Re alloying. *Acta Materialia*, 95: 456-467.
<https://doi.org/10.1016/j.actamat.2015.03.060>.
25. **Kwon, S. J.; Seo, J. W.; Jun, H. K.; Lee, D. H.** 2015. Damage evaluation regarding to contact zones of high-speed train wheel subjected to thermal fatigue, *Engineering Failure Analysis*, 55: 327-342.
<https://doi.org/10.1016/j.engfailanal.2015.07.021>.
26. **Yeter, E.** 2018. Thermal fatigue characteristics of materials used in aerospace structures. *Energy, Ecology and Environment*, 3(1): 24-31.
<https://doi.org/10.1007/s40974-017-0061-z>.
27. **Chen, C.; Wang, Y.; Ou, H.; Lin, Y. J.** 2016. Energy-based approach to thermal fatigue life of tool steels for die casting dies. *International Journal of Fatigue*, 92: 166-178.
<https://doi.org/10.1016/j.ijfatigue.2016.06.016>.
28. ANSYS manual book.
29. **Beer, F.; Johnston, E.; DeWolf, J.; Mazurek, D.; Sanghi, S.** 2014. *Mechanics of Materials* Kindle Edition.
30. **Howland, W.L.** 1936. Effect of rivet spacing on stiffened thin sheet under compression, *Journal of the Aeronautical Sciences*, 3(12): 434-439.
<https://doi.org/10.2514/8.299>.
31. **Li, D.; Han, L.; Thornton, M.; Shergold, M.** 2012. Influence of edge distance on quality and static behaviour of self-piercing riveted aluminium joints, *Materials & Design*, 34: 22-31.
<https://doi.org/10.1016/j.matdes.2011.07.046>.

E. Yeter

THERMAL FATIGUE ANALYSES OF RIVETED STRUCTURES

S u m m a r y

In this study, the effects of thermal fatigue loading on the riveted structures made of 2014, 2024, 6061 and 7075 aluminum alloys which are widely used in the aviation industry have been investigated. An algorithm has been developed under ANSYS finite element analysis software to determine the behavior of these structures that are exposed repeated thermal loading. This algorithm is based on the principle of determining the distribution of the safety factor on the material subjected to the thermal fatigue load. In the study, the rivet spacing (RS), the rivet edge distance (ED) and the rivet hole diameter (RD) were selected as riveting parameters. It is aimed to determine the optimum values of the parameters used under thermal fatigue loading and the most suitable one for this loading among the materials used. It is seen that 7075 aluminum alloy has the highest safety factor distribution for all the models in which the effect of these parameters was investigated. It has been determined that when the rivet spacing is 3 times the rivet diameter (3d), the highest safety factor value is obtained for all material types. And this value decreases when the rivet spacing is increased. When the effect of the rivet edge distance is examined, it is seen that when the rivet edge distance 8d is used, the highest safety factor value is obtained. The safety factor value is the smallest when the rivet edge distance is 2,5d. In addition, when rivet hole diameter increased from 2.5 mm to 4.8 mm, it was determined that safety factor value increased.

Keywords: thermal fatigue, riveting parameters, aluminum alloys, finite element method (FEM).

Received July 20, 2018

Accepted October 18, 2018